IOP Conf. Series: Materials Science and Engineering **219** (2017) 012051 doi:10.1088/1757-899X/219/1/012051

Orientation Dependence of the Deformation Microstructure of Ta-4%W after Cold-Rolling

J Zhang[1], G Q Ma[1], A Godfrey[2], D Y Shu[3], Q Chen[3], G L Wu[1, *]

[1] College of Materials Science and Engineering, Chongqing University, Chongqing 400045, China
[2] Key Laboratory of Advanced Materials (MoE), School of Materials Science and Engineering, Tsinghua University, Tsinghua, 100084, China
[3] Southwest Technology and Engineering Research Institute, Chongqing 400039, China

E-mail: wugl@cqu.edu.cn

Abstract: One of the common features of deformed face-centered cubic metals with medium to high stacking fault energy is the formation of geometrically necessary dislocation boundaries. The dislocation boundary arrangements in refractory metals with body-centered cubic crystal structure are, however, less well known. To address this issue a Ta-4%W alloy was cold rolled up to 70% in thickness in the present work. The resulting deformation microstructures were characterized by electron back-scattering diffraction and the dislocation boundary arrangements in each grain were revealed using sample-frame misorientation axis maps calculated using an in-house code. The maps were used to analyze the slip pattern of individual grains after rolling, revealing an orientation dependence of the slip pattern.

1. Introduction

Due to their excellent properties of high density, high corrosion resistance, high melting point, good plasticity even at low temperatures, and a moderately high elastic modulus [1-3], tantalum (Ta) and tantalum–tungsten (W) alloys are regarded as materials with great potential for high temperature applications, as well as in nuclear engineering, aerospace and other areas [4], with extensive studies have conducted on these alloys in various fields [5-7]. However, despite these studies information regarding the evolution of the deformation microstructure in Ta and Ta-W alloys is scarce. Such information regarding the dominant deformation mechanisms and the evolution of microstructure during thermo-mechanical processing is nevertheless required to help with optimization of materials properties during forming and processing.

In the past few decades many studies have been carried out on the deformation mechanism and the evolution of deformation microstructures in face centred cubic (FCC) metals [8, 9], as well as in some ferritic steels [10]. These studies have led to a framework describing the microstructure morphology in terms of dense dislocation walls, geometrically necessary boundaries (GNBs), incidental dislocation boundaries (IDBs) and lamellar boundaries (LBs). However, the evolution of deformation microstructures in refractory body-centred cubic (BCC) metals such as tantalum, where dislocation

mobility is expected to be limited at room temperature, is considerably less studied [11, 12]. The aim of this investigation is therefore to examine the deformation microstructure, and especially the GNB structure, of a Ta alloy after cold-rolling to low and medium strains.

2. Experimental

The starting material used in this study was a Ta alloy containing 4 wt.% W. The Ta-4%W alloy was prepared by an electron beam melting method. The cast rod was hot forged and annealed to obtain a recrystallized rod 50 mm in diameter. The resulting alloy had grain sizes ranging from 10 to 125 μm with an average of 26 μm, and an almost random texture. Plates of either 2 mm or 5 mm in thickness were cut from the rod, perpendicular to the hot-forging direction. The plates were then rolled at ambient temperature to reductions of 10%, 30%, 50% (initial 2 mm thickness) and 70% (initial 5 mm thickness) in a rolling mill with 150 mm diameter rollers. The specimens were cooled in cold water after each rolling pass. For electron channelling contrast (ECC) and electron backscattering diffraction (EBSD) observations, the surfaces of the specimens were mechanically ground, followed by electro-polishing in an 90ml H_2SO_4 and 10ml HF solution at room temperature for 9 minutes using a current of 0.1A/cm^2. All the ECC and EBSD experiments were conducted on the RD (rolling direction)-ND (normal direction) section. The microscope used in the present study was a JEOL 7800F scanning electron microscope (SEM) operating at 20 kV, equipped with an Oxford AZtec EBSD system.

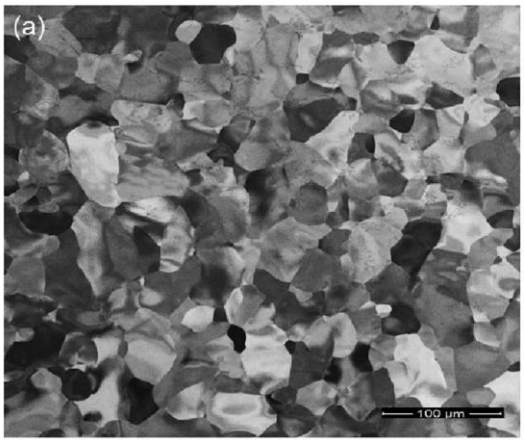

Figure 1. SEM ECC micrograph of the initial Ta-4%W alloy.

Standard EBSD orientation maps, such as inverse pole figure (IPF), directly reconstructed from experimental data, were used initially to characterize the microstructure in each sample. However, the deformation is mainly accommodated by slip in the present alloy, and many deformation features associated with dislocation slip, especially low angle dislocation boundaries, cannot be revealed clearly in IPF maps. Therefore, an in-house code was used, in which the misorientation axis in the sample reference frame of each pixel to the grain average orientation was calculated, and the resulting maps used to probe the evolution of dislocation boundaries during cold rolling [13, 14]. To construct these maps individual grains in each EBSD map were first detected and the grain average (g_{av}) orientation determined. Then the misorientation between each map pixel (g_p) and the average orientation of the grain in which it lies was calculated. Finally, an orientation map was reconstructed showing the misorientation axis, expressed in the sample coordinate frame, for each pixel in the EBSD data.

3. Results and discussion

Figure 2 shows the orientation maps of the Ta-4%W alloy after 10% rolling reduction. From the IPF map, it is seen that some grains were subdivided into several domains (figure 2a) with large orientation changes (10-15º) between neighbouring domains, and with a wide transition in orientation,

as shown by the misorientation profile (figure 2c) along the line drawn on figure 2a. The local misorientations between neighbouring points are nevertheless very small (~1° or less). Neither the IPF map, nor boundary misorientation angle maps, show a clear structure after 10% rolling. In contrast, a dislocation boundary microstructure could be readily distinguished in many grains in the sample-frame misorientation axis maps (figure 2b). In these maps it can be seen that many grains, or domains within a grain, contain either one set or two sets of well-defined dislocation boundaries inclined ±25~55° to RD. In some grains, however, dislocation boundaries are not seen.

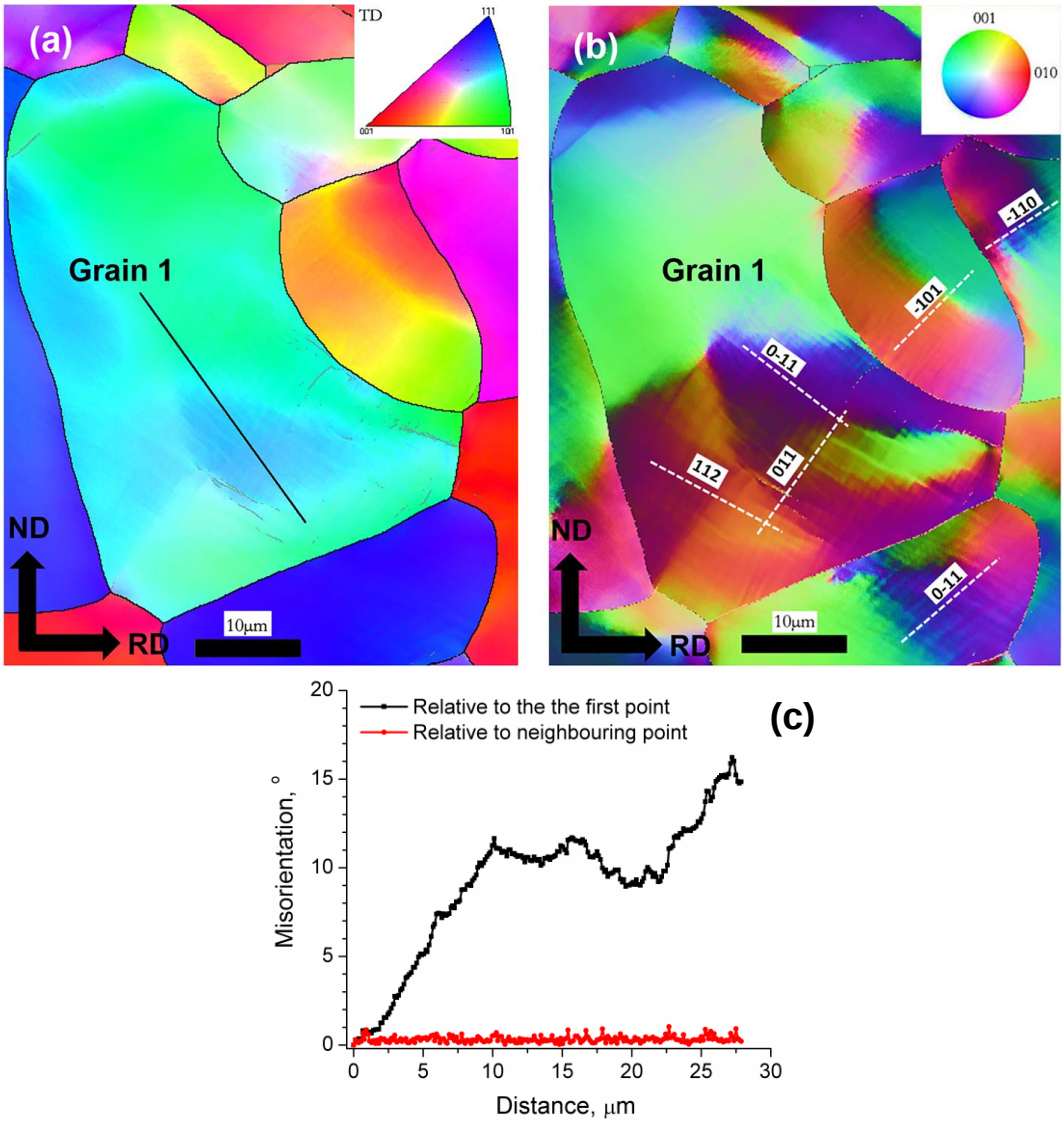

Figure 2. (a) IPF map and (b) misorientation axis map of Ta-4%W after 10% cold rolling; (c) misorientation angle versus distance along the line in (a). The colours in these figure are different, as indicated by the inserted colour scales. Black lines represent misorientation angles ≥ 15 °, and grey lines ≥ 2 ° and < 15 °.

For each grain where well defined dislocation boundaries were seen, the traces of {110} and {112} slip planes on the longitudinal section were calculated. If the trace of a slip plane is within 5° to a dislocation boundary on the misorientation axis map, it is assumed that this slip system was strongly activated during cold rolling producing the dislocation boundary. In this manner all the visible

dislocation boundaries were examined. Some examples of active slip traces are also shown on the map in figure 2b. For the grain 1, the slip traces of two neighbouring domains are identified as (011) & (0-11) and (011) & (112), respectively. Therefore, the activated slip systems of these two neighbouring domains are different, and can be attributed to the difference in orientation between these regions

Figure 3a and 3b are the IPF and the misorientation axis maps after rolling to 30% reduction. A similar deformation microstructure to that seen at 10% rolling is seen. However, a larger density of low angle misorientation boundaries is now seen in the microstructure. Additionally, more grains or domains are observed containing two sets of dislocation boundaries. These dislocation boundaries are aligned about ±15~50° to RD, and are again found to be mostly parallel to the slip traces of {110} or {112} planes. Domains inside grains can also be found, with the transition regions between domains much narrower than at the lower strain. One example is shown in figure 3c, which gives the misorientation versus distance along the line on figure 3a. The local misorientations vary typically from 2-7°. The misorientation between two neighbouring domains can, however, be as large as 20-25°, with this large orientation change occurring over a distance of ~1.5 μm. The pole figure for the region indicated by a circle in figure 3a, which contains the two domains, shows that these domains are rotated in opposite directions about a common [110] axis (as indicated by the circle in figure 3d), which is also approximately parallel to the TD. The misorientation changes across some transition regions are so abrupt that high angle boundaries can be formed between neighbouring domains, as indicated by arrows in grain 2 on figure 3a.

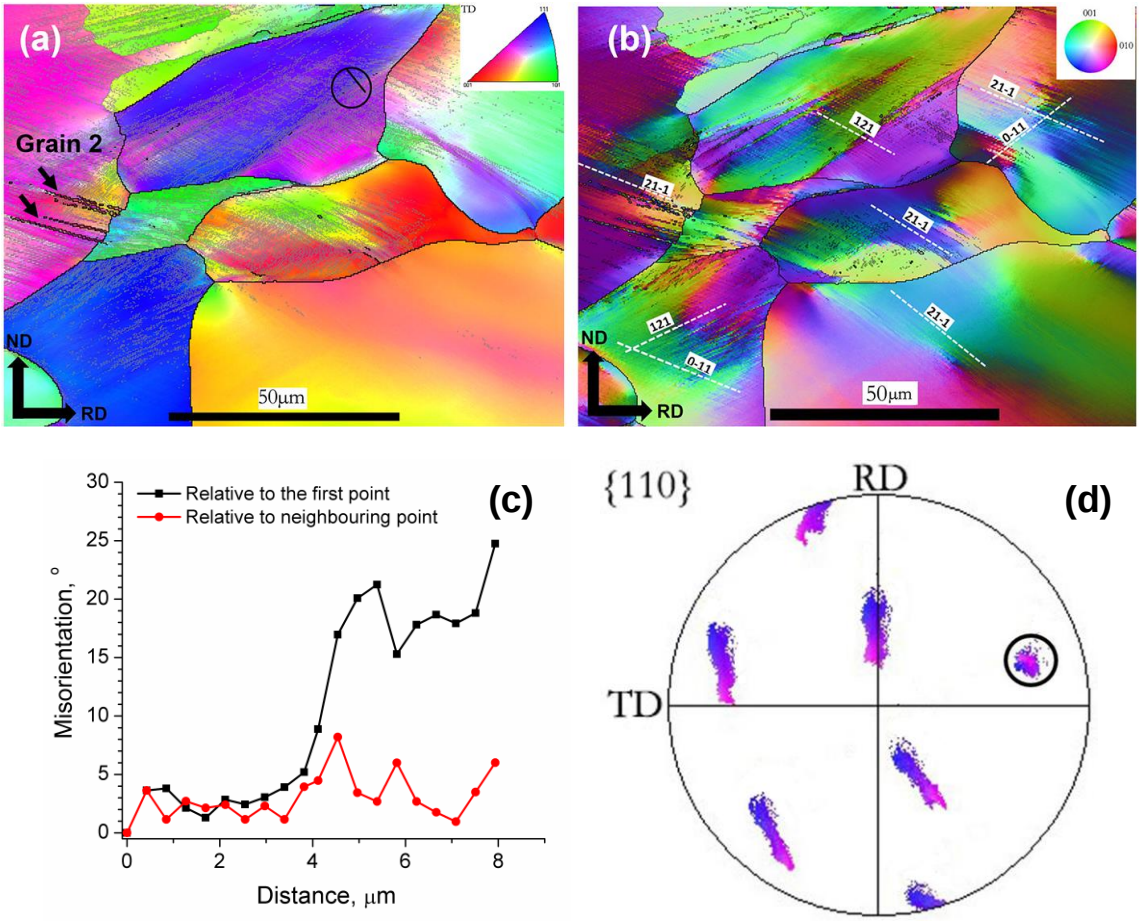

Figure 3. (a) IPF and (b) misorientation axis map of Ta-4%W after 30% cold rolling; (c) misorientation angle versus distance along the line on (a); (d) {110} pole figure of the data inside the circle in (a).

Figures 4a and 4b show the IPF map and rotation axis map of the 50% cold rolled sample. It is seen that many grains are elongated along RD. Many grains or domains contain well-defined dislocation boundaries and some grains or domains with large sizes only have low angle dislocation boundaries. The dislocation boundaries are aligned ±10~50° to RD. Some example slip traces of these boundaries are shown in figure 4b. Fragmented areas containing high angle boundaries to neighbouring regions are also observed in a number of places. These fragmented areas are believed to be created by further development of the rapid orientation changes across neighbouring domains as seen in the sample after 30% rolling.

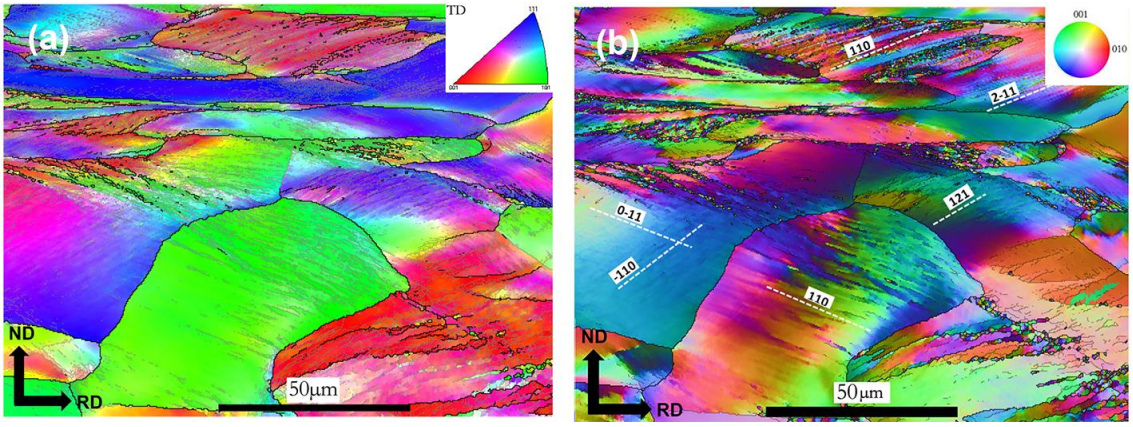

Figure 4. (a) IPF and (b) misorientation axes map of the Ta-4%W after 50% cold rolling.

After 70% cold rolling reduction, the original grains are very clearly elongated and it becomes much more difficult to clearly distinguish features in the more complicated microstructure seen at this strain. Well-defined dislocation boundaries can, nevertheless, still be recognized in many grains and domains. Such dislocation boundaries are inclined ±10~45° to RD, and in many case are close to slip traces (figure 5a). S-shaped bands are also seen in the 70% rolled sample. The formation of S-bands (as shown in figure 5b) is a result of the intersection of two dislocation boundaries, in which localized micro-shearing takes place. The dislocation boundaries in some areas are disturbed, being bent towards original grain boundaries (as shown in figure 5c). Accordingly, in these regions the boundaries are typically no longer parallel to the traces of {110} or {112} planes.

In total, 110 grains were examined in the present experiment. Grains containing either one or two sets of well-defined dislocation boundaries were observed in all examined specimens. The observed dislocation boundaries are believed to be GNBs, as seen previously in FCC (i.e. Al, Ni, Cu) metals and IF steel, where their formation has been extensively studied. The present results for Ta-W alloy (as a BCC refractory metal with a very high melting point and a high stacking fault energy) are similar to those found for IF steel, in which the GNBs were found parallel to either {110} or {112} slip traces.

One interesting point for the GNB structure in the present results is that the local misorientation is quite small after deformation to 10% and 30% so that the GNB structure cannot be revealed very clearly, even in the sample-frame misorientation axis maps. However, the orientation gradients are very large, ~1°/μm and 10°/μm for the two examples in figures 2c and 3c, respectively. Such a large orientation gradient indicates a dislocation density that is very high to accommodate the lattice curvature. However, due to high melting point of this material these dislocations are not able to dynamically recover during plastic deformation by the heat generated by rolling processing. As such it is expected that the dislocation boundaries will not be as narrow (sharp) as seen in deformed Al alloys, but more similar to those seen in Ni. This will be further explored by transmission electron microscopy studies.

In the present results, many of the dislocation boundaries are parallel to the traces of {110} or {112} slip planes, presumed to be active during rolling. For all the grains or domains having identified

dislocation boundaries inside, the Schmid factors of all {110} and {112} slip systems were calculated, according to the average orientation of the region where they were found after deformation. It was found that the slip systems corresponding to the observed slip traces do not always have the maximum Schmid factors, but always correspond to one of the slip systems with the largest three Schmid factors. Similar results were also found in IF steel during cold rolling.

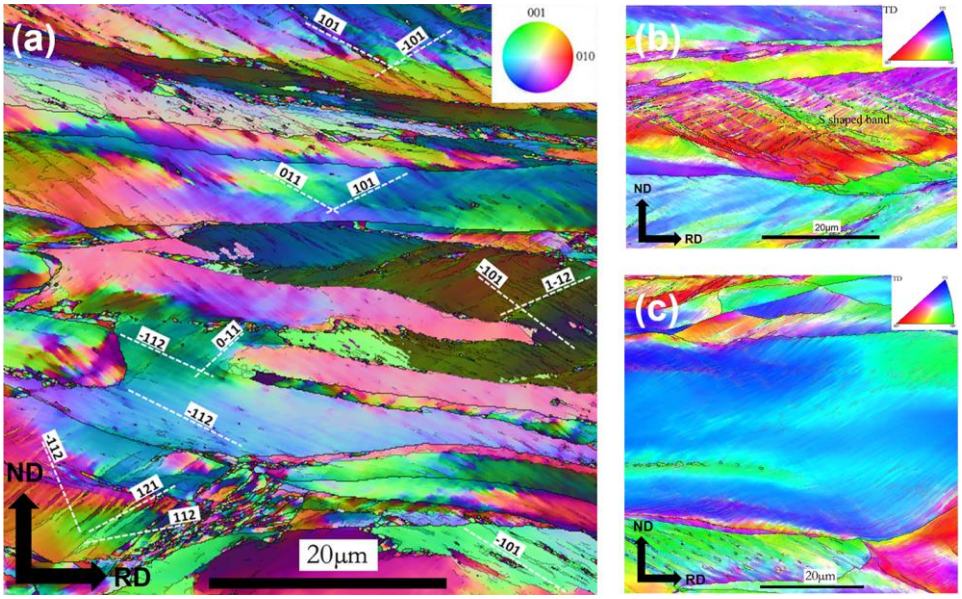

Figure 5. (a) Misorientation axis map of Ta-4%W after 70% cold rolling; (b) IPF map showing the S shaped bands; (c) IPF map showing distorted dislocation boundaries in near-grain boundary regions.

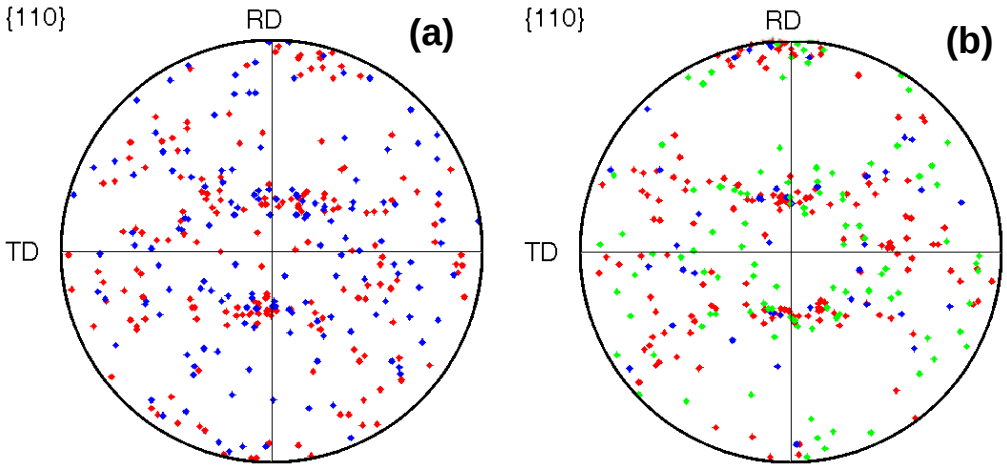

Figure 6. Pole figure showing grains with (a) one set and (b) two sets of dislocation boundaries. In the pole figure, red points represent GNBs close only to {110} traces; blue only to {112} traces, and green for type B grains where one set is close to a {110} trace and the other to a {112} trace.

In earlier studies of rolled Al and Cu a clear relationship between dislocation pattern and grain orientations was found. In the present study the grains or domains where dislocation boundaries are clearly seen are classified into two types: (i) type A (containing one set of GNB), and (ii) type B (containing two sets of GNBs). The orientations associated with each type are shown in figure 6. It is seen that the orientations of grains having type A structure are rather random. In contrast, the grains with type B structure have orientations belonging to the α-fibre (<110> || RD). The results demonstrate therefore an orientation dependence of slip pattern in rolled Ta-4%W. For grains with one set of GNBs, the orientations of the grains where boundaries are close to a {110} slip plane and a {112} slip plane are similar. For type B grains in most cases the GNBs are both close to {110} slip planes. Type B grains with GNBs near to two sets of {112} boundaries are only observed after 70% rolling.

In this investigation only the GNBs have been characterized. IDBs, as observed in deformed FCC metals by using transmission electron microscopy, cannot be determined in the present experimental because of the limited resolution of the EBSD technique. The density and arrangements of these boundaries are however also important and will be studied in future work.

4. Conclusions

A Ta-4%W alloy has been cold rolled to strains of 10% to 70%. The deformation microstructures after each rolling strain were characterized by the EBSD technique, and dislocation boundaries were revealed using an in-house code to plot maps showing the misorientation axis of each pixel to grain average in the sample reference frame. It is found that:

1. Grains develop one set or two sets of dislocation boundaries after rolling and the dislocation boundaries are typically parallel to {110} or {112} slip planes;
2. The grains having one set of dislocation boundary have random orientations, while grains having two sets of dislocation boundaries belong to the α-fibre.

Acknowledgments

This work was supported by the National Natural Science Foundation of China (51471039) and State Key Research and Development Program of China (2016YFB0700403).

References

[1] Kaufmann D, Mönig R, Volkert CA, Kraft O 2011 *Inter. J. Plast.* **27** 470
[2] Hupalo MF, Sandim HRZ 2001 *Mater. Sci. Eng. A* **318** 216
[3] Zhou JQ, Khan AS, Cai R, Chen L 2006 *J. Iron Steel Res.* **13** 68
[4] Kuznietz M, Livne Z, Cotler C, Erez G 1998 *J. Nucl. Mater.* **152** 235
[5] Deng C, Liu SF, Ji JL, et al 2014 *J Mater. Proc. Tech.* **214** 462
[6] Nesterenko VF, Meyers MA, LaSalvia JC, et al 1997 *Mater. Sci. Eng. A* **229** 23
[7] ElAbedin SZ, Welz-Biermann U, Endres F 2005 *Electrochemistry Commun.* **7** 941
[8] Liu Q, Hansen N 1995 *Scripta Metall. Mater.* **32** 1289
[9] Liu Q, Juul Jensen D, Hansen N 1998 *Acta Mater.* **46** 5819
[10] Li BL, Godfrey A, Meng QC, Liu Q, Hansen N 2004 *Acta. Mater.* **52** 1069
[11] Wang S, Chen C, Jia YL, et al 2016 *Int. J. Refract. Metals Hard Mater.* **54** 104
[12] Moussa C, Bernacki M, Besnard R, Bozzolo N 2015 *IOP Conf. Ser.: Mater. Sci. Eng.* in *Proc. of 36th Risø Inter. Sym. on Mater. Sci.* **89** 012038
[13] Hong X, Godfrey A, Zhang CL, Liu W, Chapuis A 2017 *Mater. Sci. Eng. A* **693** 14
[14] Albou A, Driver JH, Maurice C 2010 *Acta Mater.* **58** 3022